The Effect of Imperfect Feedback on Age-Threshold Slotted ALOHA

Runze Jin*§, Fangming Zhao*§, Nikolaos Pappas†, Yi Zhong‡, Howard H. Yang*§

*ZJU-UIUC Institute, Zhejiang University, China
†Department of Computer and Information Science, Linköping University, Sweden
‡School of Electronic Information and Communications, Huazhong University of Science and Technology, China
§National Mobile Communications Research Laboratory, Southeast University, China
runze.23@intl.zju.edu.cn, fangming.23@intl.zju.edu.cn, nikolaos.pappas@liu.se, yzhong@hust.edu.cn, haoyang@intl.zju.edu.cn

***Abstract*—We analyze the age-threshold slotted ALOHA (TSA) protocol in a Poisson cellular network, considering potential ACK feedback errors. In this setup, spatially distributed nodes must update their status information to a designated access point over a shared spectrum. The TSA protocol requires source nodes to remain silent until their local Age of Information (AoI) reaches a preset threshold, after which each node independently decides whether to transmit in the current time slot with a certain probability. With imperfect ACK feedback, the source node may fail to reset its local AoI when ACK feedback error occur, causing the age-threshold policy to become temporarily ineffective. Based on this setting, we derive analytical expressions for the transmission success probability and the network average AoI. Our findings demonstrate that imperfect ACK feedback significantly affects the performance limits of network average AoI when employing the TSA protocol.**

***Index Terms*—Age of information, Poisson cellular networks, age-threshold, Imperfect feedback.**

I. Introduction

The efficiency of Internet of Things (IoT) services, such as smart homes, smart cities, and intelligent healthcare, relies on the timeliness of information delivery. As a result, ensuring the timely delivery of information in these applications has emerged as an important research topic [1]. The Age of Information (AoI) and its recent variants provide a performance metric to quantify the freshness of information, thereby presenting ample opportunities to improve the performance of real-time network applications [2], [3].

Owing to the natural requirement for low implementation cost and large-scale deployment, IoT networks normally constitute random access architecture, in which the nodes are randomly distributed, and centralized coordination is lacking, while network scalability is needed. An appropriate analytical framework can offer valuable insights into network design by optimizing AoI. In this paper, we carry out an analytical study, aiming to advance the understanding of age-threshold slotted ALOHA (TSA), a variant of the traditional slotted ALOHA (SA) protocol that enhances the timeliness of random access networks, with a particular focus on the quality of ACK feedback on the performance of this scheme.

This paper is supported in part by the National Natural Science Foundation of China under Grant 62201504, in part by the open research fund of National Mobile Communications Research Laboratory, Southeast University (No. 2024D05), and in part by the Zhejiang Provincial Natural Science Foundation of China under Grant LGJ22F010001, and in part by the National Natural Science Foundation of China (NSFC) grant No. 62071190. (*Corresponding Author:* Howard H. Yang)

A. Related Works

To enhance AoI in random access networks, researchers often perform analysis and optimization on the basis of the SA protocol. Specifically, authors in [4] optimize the channel access probability of each source node and the sampling rate to minimize the mean peak AoI at the receiver. The authors in [5] optimize the AoI for both scheduled access and a slotted ALOHA-like random access. The authors in [6] establish a spatiotemporal model to characterize the AoI by combining queueing theory and stochastic geometric. In [7], the authors provide tractable expressions for both the peak and average AoI under first-come-first-serve (FCFS) and last-come-first-serve with preemption (LCFS-PR) policies, respectively. The authors in [8] focus on reducing interference among geographically close transmitters to minimize the network average AoI, while authors in [9] propose a frame slotted ALOHA-based protocol to minimize the network average AoI and its variance.

Inspired by the fact that stipulating a waiting period at the source node usually benefits AoI [10], researchers have recently explored the TSA protocol to further optimize the AoI performance metric. For instance, the authors in [11] introduce a threshold-based age-dependent random access (ADRA) protocol, where each source node accesses the channel with a specific probability only when its instantaneous AoI exceeds a preset threshold. The authors in [12] introduce the age-gain for information packets, with transmitters operating in a decentralized manner based on the age-gain of update packets. In [13], the author presents mini-slotted threshold ALOHA (MiSTA), a variant of TSA aimed at reducing the network average AoI over time. The authors in [14] propose an age threshold-based dynamic frame slotted ALOHA for resolving contention in random access networks. The authors in [15]

ISBN 978-3-903176-65-2 © 2024 IFIP

TABLE I: NOTATIONS SUMMARY

Notations	Definition	Notations	Definition
Φ_s	Stationary and ergodic point process modeling the locations of souces	Φ_d	Stationary and ergodic point process modeling the locations of destinations
λ_s	Source spatial deployment density	λ_d	Destination spatial deployment density
ϵ	ACK feedback failure probability	η	Packet update rate
A	Age-threshold	$\|x_i\|$	Distance between source i and the typical receiver
x_i	Position of source i	θ	SIR decoding threshold
$\|x_0\|$	Distance of typical transmitter-receiver pair	α	Path loss exponent
v_i	State indicator of source i	h_i	channel fading from transmitter i to the typical receiver
μ_0^Φ	Transmission success probability	$\bar{\Delta}$	Network average AoI

demonstrate that in densely deployed networks, implementing TSA can significantly reduce the network average AoI. In [16], closed-form expressions are derived for the optimal update rate and age threshold that minimize the mean peak and time-average AoI in mobile Poisson bipolar networks.

The existing research on the TSA protocol has primarily focused on how the age threshold affects AoI, with most studies assuming perfect ACK feedback. However, since the AoI metric is defined at the destination node while the age threshold policy is implemented at the transmitter, an ACK feedback decoding failure may prevent the source node from resetting its local AoI count to synchronize with the destination node, rendering the age-threshold policy temporarily ineffective. Therefore, the impact of ACK feedback decoding failures on the AoI metric under the TSA protocol warrants further discussion. In this paper, we conduct an AoI analysis of the TSA protocol in Poisson cellular networks, with a particular focus on the effect of imperfect ACK feedback. This approach enables us to obtain useful insights for the design of TSA random access networks.

B. Contributions

The main contributions of this paper are summarized below.

- We develop a mathematical framework for analyzing the impact of the TSA protocol on the AoI performance of Poisson cellular networks with imperfect ACK feedback. We establish a fixed-point equation to characterize the transmission success probability, encompassing key features such as ACK feedback failure probability, update rate, age threshold, channel fading, deployment density, and co-channel interference.
- We derive analytical expressions for the network average AoI under conditions of imperfect ACK feedback. The results indicate that when ACK feedback failures are considered, the network average AoI is much higher than in scenarios with perfect ACK feedback. This is because the function of TSA to reduce interference and equalize the update intervals are less effective.
- Our analysis revealed that when imperfect ACK feedback is considered, the TSA effectively becomes a hybrid of the TSA and SA protocols, resulting in performance loss. While appropriately increasing the age threshold can help mitigate this performance loss, it still remains slightly worse than in the perfect ACK feedback scenario.

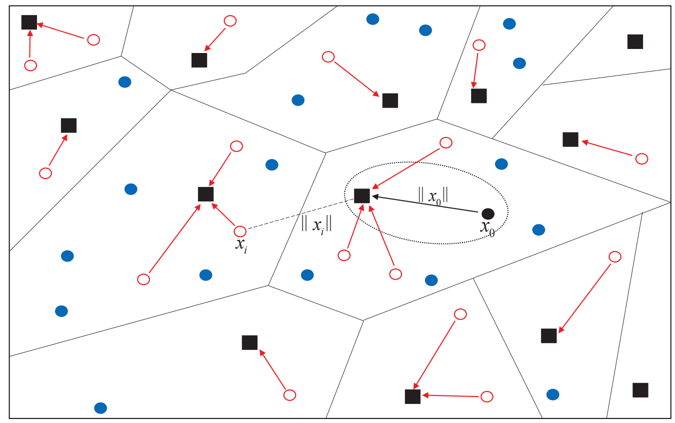

Fig. 1: An example of the Poisson cellular network, where the sources and destinations are denoted by the circles and squares, respectively. The solid blue circles are inactive sources with no connection.

II. SYSTEM MODEL

A. Spatial Configuration

We consider a Poisson cellular network consisting of source and destination nodes, as depicted in Fig. 1. The spatial positions of the sources and their destinations are modeled by stationary and ergodic point processes, denoted by Φ_s and Φ_d, respectively. The source nodes are scattered as a homogeneous PPP Φ_s of intensity λ_s. The destination nodes are deployed according to an independent homogeneous PPP Φ_d with spatial density λ_d. Every source node is associated with the closest destination nodes in the geographical vicinity. A sequence of status information is generated at each source, encapsulated into information packets, and transmitted over a shared spectrum. When a source node sends out information packets, it transmits at a fixed power. We assume the channel between any pair of nodes is affected by the Rayleigh fading with a unit mean, which varies independently across time slots, and path loss that follows the power law.

B. Temporal Attribute

We consider a discrete-time system where the time is segmented into equal-length durations. We assume the network is synchronized. We employ the TSA protocol for status updating, as illustrated in Fig. 2. Specifically, each source node remains inactive until its AoI reaches a predefined threshold, denoted by A. After that, every source independently decides

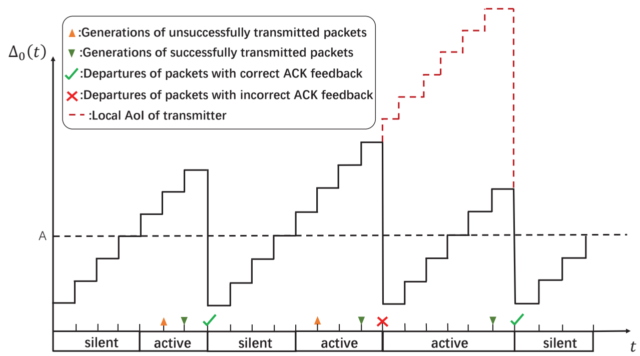

Fig. 2: An example of AoI evolution over the link under the TSA status updating protocol with imperfect ACK feedback.

whether it will update in this slot or not, at the beginning of each subsequent time slot, with probability η; if a source decides to update in this time slot, the source node generates a new update and immediately transmits the information packet to the destination. If the received signal-to-interfernce ratio exceeds the decoding threshold θ, the transmission is successful. Subsequently, the destination node feeds an ACK back to the source, where the transmission fails with probability ϵ. Upon receiving the ACK, the source resets the local age to one.

C. Performance Metric

We use AoI to quantify the freshness of information delivered in this network. Formally, the AoI evolution over the typical link can be written as follows:

$$\Delta_0(t) = t - G_0(t), \tag{1}$$

where $G_0(t)$ indicates the time-stamp of the most recent update received by the typical destination at time t. In this paper, we employ the network average AoI as our performance metric. Specifically, we denote by $\Delta_j(t)$ the instantaneous AoI of link j at time slot t. Then, the time-average AoI over this link is

$$\bar{\Delta}_j = \lim_{n\to\infty} \frac{1}{T} \sum_{t=1}^{T} \Delta_j(t), \tag{2}$$

and the network average AoI is defined as

$$\bar{\Delta} = \lim_{R\to\infty} \sup \frac{\sum_{j:X_j\in B(o,R)} \bar{\Delta}_j(t)}{\lambda\pi R^2}, \tag{3}$$

where $B(o,R)$ denotes a disk centered at the origin with radius R. Since the point processes under the TSA protocol still exhibit ergodicity and stationarity, we have $\bar{\Delta} = \mathbb{E}\left[\bar{\Delta}_0\right]$.

III. Analysis

We consider an interference-limited scenario and adopt signal-to-interfernce ratio (SIR) to evaluate the transmission quality of wireless links. If the typical source node, situated at x_0, transmits a packet to its intended destination node at a time slot t, the received SIR can be written as:

$$\mathrm{SIR}_0(t) = \frac{h_{00}(t)\|x_0\|^{-\alpha}}{\sum_{i\neq 0} h_{i0}(t) v_i(t) \|x_i\|^{-\alpha}}, \tag{4}$$

where $h_{i0}(t) \sim \exp(1)$ represents the channel fading from source node i to the typical destination node, α is the path loss exponent, $\|\cdot\|$stands for the Euclidean norm, and $v_i(t)$ is a binary function, where $v_i(t) = 1$ if source node i is active and $v_i(t) = 0$ otherwise.

According to the decoding criteria, given point process $\Phi = \Phi_{\mathrm{s}} \cup \Phi_{\mathrm{d}}$, the conditional probability of successfully transmitting a packet from the typical source node can be written as

$$\mu_0^{\Phi} = \mathbb{P}(\mathrm{SIR}_0 > \theta \big| \Phi), \tag{5}$$

where θ is the decoding threshold of information packet.

In what follows, we analyze the network average AoI under TSA based on the distribution of $\mathrm{SIR}_0(t)$. Since the point process is stationary, we drop the time index in the sequel. We start the analysis by deriving each node's active probability.

A. Node Active Probability

We focus on the typical source node and model the dynamics of its local AoI by a discrete-time Markov chain with state space $\mathcal{A} = \{1,2,3,...A,...\} \bigcup \{\text{AckFailed}\}$, illustrated in Fig. 3. We denote by ω the state (i.e., local AoI) of the source node. When $\omega \in \{1,2,3,...A,...\}$, the AoI count in the source and destination nodes are synchronized; when $\omega \in \{\text{AckFailed}\}$, the AoI of source node and destination node are not synchronized because of the ACK feedback failure. As such, a typical source node may experience the following transition in a generic time slot:

- If $\omega \in [1, A-1]$, the source node is silent, and $\omega \to \omega+1$ with probability 1 in the next time slot.
- If $\omega \in [A, \infty)$, the source node can be active because the local AoI count exceeds the age threshold. Then, three transitions are possible:
  1) $\omega \to \omega+1$: If the source node does not transmit or the transmission fails, which happens with probability $1 - \eta\mu_0^{\Phi}$.
  2) $\omega \to 1$: If the transmission succeeds and the ACK feedback is correctly decoded, which happens with probability $(1-\epsilon)\eta\mu_0^{\Phi}$.
  3) $\omega \to \{\text{AckFailed}\}$: If the transmission succeeds but the ACK feedback is incorrectly received, which happens with probability $\epsilon\eta\mu_0^{\Phi}$.
- If $\omega \in \{\text{AckFailed}\}$, the activation of a source node is due to the asynchronization between the source node. In this case, two transitions are possible:
  1) $\omega \to 1$: If the transmission is successful and the ACK is correct, which occurs with probability $(1-\epsilon)\eta\mu_0^{\Phi}$.
  2) $\omega \to \{\text{AckFailed}\}$: This happens when (i) the source node does not transmit, or (ii) the source node transmits but the transmission fails, or (iii) the transmission is successful but the ACK feedback fails, the corresponding probability is $1 - \epsilon\eta\mu_0^{\Phi}$.

Consequently, we denote by S_i the probability of the state of the source node being i, namely, $S_i = \mathbb{P}(\omega = i)$. The

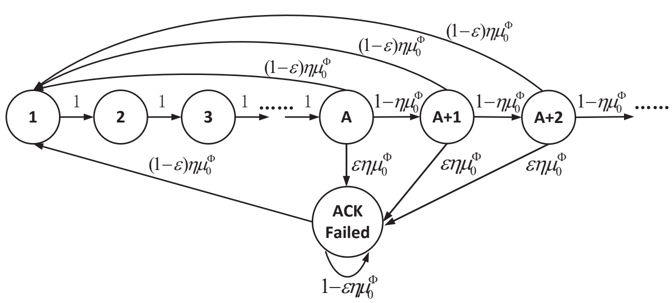

Fig. 3: A Markov chain characterization of the local AoI transitions in the (potentially) incorrect ACK feedback case.

steady-state probability equations are given as:

$$\begin{cases} S_1 = S_2 = \ldots = S_A, \\ S_{\text{AckFailed}} = \epsilon \sum_{i=A}^{\infty} S_i + (1-\epsilon\eta\mu_0^\Phi) S_{\text{AckFailed}}, \\ S_{A+i} = (1-\eta\mu_0^\Phi)^i S_A, \\ S_1 = \eta\mu_0^\Phi (1-\epsilon) S_{\text{AckFailed}} + \eta\mu_0^\Phi (1-\epsilon) \sum_{i=A}^{\infty} S_i. \end{cases} \tag{6}$$

Since $\sum_{i=1}^{\infty} S_i + S_{\text{AckFailed}} = 1$, the active probability of a generic source node j can be obtained as

$$\begin{aligned} a_j^\Phi &= \mathbb{P}(v_j = 1) \\ &= \eta \left(\sum_{i=A}^{\infty} S_i + S_{\text{AckFailed}} \right) = \frac{\eta}{A\eta\mu_j^\Phi(1-\epsilon)+1}. \end{aligned} \tag{7}$$

The analysis in (7) indicates that, under TSA protocol, the active probability of each node increases with the ACK feedback failure probability rises. This is because when the ACK feedback fails, the source node is unable to reset the local age and thus does not enter the silent period.

B. Conditional Transmission Success Probability

Given the network topology, we begin by averaging out the randomness in channel fading in the transmission success probability, as follows.

Lemma 1. *Conditioned on the network topology, the transmission success probability under TSA with imperfect ACK feedback is given by*

$$\mu_0^\Phi = \prod_{i \neq 0} \left(1 - \frac{\frac{\eta}{1+A\eta\mu_i^\Phi(1-\epsilon)}}{1 + \frac{\|x_i\|^\alpha}{\theta\|x_0\|^\alpha}} \right). \tag{8}$$

Proof. The transmission success probability can be derived as

$$\begin{aligned} \mu_0^\Phi &= \mathbb{P}\left(\frac{h_{00}\|x_0\|^{-\alpha}}{\sum_{i\neq 0} h_{i0} v_i \|x_i\|^{-\alpha}} > \theta \middle| \Phi \right) \\ &= \mathbb{E}\left[\prod_{i\neq 0} \exp\left(-\theta h_{i0} v_i \|x_0\|^\alpha \|x_i\|^{-\alpha}\right) \middle| \Phi \right] \\ &\overset{(a)}{=} \mathbb{E}\left[\prod_{i\neq 0} \left(\frac{1}{1+\theta\|x_0\|^\alpha v_i \|x_i\|^{-\alpha}} \right) \middle| \Phi \right] \\ &\overset{(b)}{=} \prod_{i\neq 0} \left(1 - \frac{a_i^\Phi}{1+\frac{\|x_i\|^\alpha}{\theta\|x_0\|^\alpha}} \right), \end{aligned} \tag{9}$$

where (a) follows since $\{h_{i0}\}_i^\infty$ are i.i.d. pace random variables following the exponential distribution with unit mean, and (b) follows as $\{v_i\}_i^\infty$ are independent of each other. Then, the result can be obtained by involving the analytical expression of the node active probability in (7). □

Next, we derive the analytical expression of the conditional transmission success probability.

Theorem 1. *The cumulative distribution function (CDF) of the conditional transmission success probability is given by the fixed-point eqaution (10) at the top of the next page, in which $j = \sqrt{-1}$ and $\mathrm{Im}\{\cdot\}$ denotes the imaginary part of a complex quantity, while $B\left(\frac{2}{\alpha}, k-\frac{2}{\alpha}\right)$ is the Beta function, given by*

$$B\left(\frac{2}{\alpha}, k-\frac{2}{\alpha}\right) = \int_0^1 \zeta^{\frac{2}{\alpha}-1}(1-\zeta)^{k-\frac{2}{\alpha}-1} \mathrm{d}\zeta. \tag{11}$$

Proof. Please see the Appendix A. □

Notably, the probability density function (PDF) of μ_0^Φ can be tightly approximated by the following:

$$f(x) = \lim_{n\to\infty} f_n(x) = \lim_{n\to\infty} \frac{x^{a_n-1}(1-x)^{b_n-1}}{B(a_n,b_n)}, \tag{12}$$

where $B(a_n,b_n)$ denotes the Beta function, given by

$$B(a_n,b_n) = \int_0^1 \zeta^{a_n-1}(1-\zeta)^{b_n-1} \mathrm{d}\zeta, \tag{13}$$

and a_n and b_n are respectively matching the mean and variance of μ_0^Φ. Specifically, these two quantities can be obtained as

$$\frac{a_n}{a_n+b_n} = \mathbb{E}\left[\mu_0^\Phi\right], \tag{14}$$

$$\frac{a_n b_n}{(a_n+b_n)^2(a_n+b_n+1)} = \mathbb{E}\left[(\mu_0^\Phi)^2\right] - \left(\mathbb{E}\left[\mu_0^\Phi\right]\right)^2. \tag{15}$$

After calculation, a_n and b_n can be get as follows:

$$a_n = \frac{\mathbb{E}\left[\mu_0^\Phi\right]\left(\mathbb{E}\left[\mu_0^\Phi\right] - \mathbb{E}\left[(\mu_0^\Phi)^2\right]\right)}{\mathbb{E}\left[(\mu_0^\Phi)^2\right] - \left(\mathbb{E}\left[\mu_0^\Phi\right]\right)^2}, \tag{16}$$

and

$$b_n = \frac{\left(1-\mathbb{E}\left[\mu_0^\Phi\right]\right)\left(\mathbb{E}\left[\mu_0^\Phi\right] - \mathbb{E}\left[(\mu_0^\Phi)^2\right]\right)}{\mathbb{E}\left[(\mu_0^\Phi)^2\right] - \left(\mathbb{E}\left[\mu_0^\Phi\right]\right)^2}, \tag{17}$$

in which $\mathbb{E}[\mu_0^\Phi]$ can be computed by taking $m=1$ in (25), that is:

$$\mathbb{E}\left[\mu_0^\Phi\right] = \frac{1}{1 + \frac{\frac{8}{5}\lambda_s\theta^{\frac{2}{\alpha}}}{\lambda_d\alpha}\mathbb{E}\left[\frac{\eta}{1+A\eta\mu_0^\Phi(1-\epsilon)}\right] B\left(\frac{2}{\alpha}, 1-\frac{2}{\alpha}\right)}, \tag{18}$$

and $\mathbb{E}[(\mu_0^\Phi)^2]$ is the special case of (25) when $m=2$, which presents in (19) at the top of next page.

C. AoI Analysis

Let us denote by J_k the waiting time at the destination between successful receptions of the k_{th} and $(k+1)_{th}$ updates,

$$F(u)=\frac{1}{2}-\int_0^{\infty}\mathrm{Im}\left\{\exp\left(-j\omega\log u-\frac{1}{1+\frac{\frac{8}{5}\lambda_s\theta^{\frac{2}{\alpha}}}{\lambda_d\alpha}B\left(\frac{2}{\alpha},k-\frac{2}{\alpha}\right)\sum_{k=1}^{\infty}\binom{j\omega}{k}\int_0^1\frac{(-1)^{k+1}\eta^k F(\mathrm{d}s)}{(1+A\eta s(1-\epsilon))^k}}\right)\right\}\frac{\mathrm{d}\omega}{\pi\omega} \tag{10}$$

$$\mathbb{E}\left[(\mu_0^{\Phi})^2\right]=\frac{1}{1+\frac{\frac{8}{5}\lambda_s\theta^{\frac{2}{\alpha}}}{\lambda_d\alpha}\left(2\mathbb{E}\left[\frac{\eta}{1+A\eta\mu_0^{\Phi}(1-\epsilon)}\right]B\left(\frac{2}{\alpha},1-\frac{2}{\alpha}\right)-\mathbb{E}\left[\left(\frac{\eta}{1+A\eta\mu_0^{\Phi}(1-\epsilon)}\right)^2\right]B\left(\frac{2}{\alpha},2-\frac{2}{\alpha}\right)\right)}. \tag{19}$$

---

respectively. The time-average AoI over the typical link can be calculated as [15]:

$$\bar{\Delta}_0=\frac{\mathbb{E}\left[J_k^2\right]}{2\mathbb{E}\left[J_k\right]}+\frac{1}{2}. \tag{20}$$

Since the transmission success probability μ_0^{Φ} is i.i.d over the time, we can compute $\mathbb{E}\left[J_k\right]$ and $\mathbb{E}\left[J_k^2\right]$ as the following:

$$\begin{aligned}\mathbb{E}\left[J_k\right]&=(1-\epsilon)\,\mathbb{E}\left[J_k|\mathrm{TSA}\right]+\epsilon\mathbb{E}\left[J_k|\mathrm{SA}\right]\\&=(1-\epsilon)\left(A+\sum_{n=1}^{\infty}\mathbb{E}\left[n\mu_0^{\Phi}\left(1-\mu_0^{\Phi}\right)^{n-1}\right]\right)\\&\qquad+\epsilon\sum_{n=1}^{\infty}\mathbb{E}\left[n\mu_0^{\Phi}\left(1-\mu_0^{\Phi}\right)^{n-1}\right]\\&=(1-\epsilon)\left(A+\frac{\mathbb{E}\left[I_n\right]}{\mu_0^{\Phi}}\right)+\epsilon\frac{\mathbb{E}\left[I_n\right]}{\mu_0^{\Phi}},\end{aligned} \tag{21}$$

and

$$\begin{aligned}\mathbb{E}\left[J_k^2\right]&=(1-\epsilon)\,\mathbb{E}\left[J_k^2|\mathrm{TSA}\right]+\epsilon\mathbb{E}\left[J_k^2|\mathrm{SA}\right]\\&=(1-\epsilon)\left(A^2+2A\mathbb{E}\left[\sum_{n=1}^{N}I_n\right]+\mathbb{E}\left[\left(\sum_{n=1}^{N}I_n\right)^2\right]\right)\\&\qquad+\epsilon\left(\mathbb{E}\left[\left(\sum_{n=1}^{N}I_n\right)^2\right]\right)\\&=(1-\epsilon)\left(A^2+\frac{2A\mathbb{E}\left[I_n\right]+\mathbb{E}\left[I_n^2\right]}{\mu_0^{\Phi}}+\frac{2\left(1-\mu_0^{\Phi}\right)\left(\mathbb{E}\left[I_n\right]\right)^2}{\left(\mu_0^{\Phi}\right)^2}\right)\\&\qquad+\epsilon\left(\frac{\mathbb{E}\left[I_n^2\right]}{\mu_0^{\Phi}}+\frac{2\left(1-\mu_0^{\Phi}\right)\left(\mathbb{E}\left[I_n\right]\right)^2}{\left(\mu_0^{\Phi}\right)^2}\right),\end{aligned} \tag{22}$$

where I_n is the time interval between two consecutive transmission attempts over the typical link. When a source node is allowed to transmit, it generates new updates with probability η independently over time, We have $\mathbb{E}[I_n]=\frac{1}{\eta}$ and $\mathbb{E}[I_n^2]=\frac{2-\eta}{\eta^2}$.

Combining the above equations, we obtain the analytical expression of the network average AoI as follows.

Theorem 2. *Under the TSA protocol, the network average AoI in the presence of ACK feedback failures is*

$$\bar{\Delta}=\frac{1}{\eta}\mathbb{E}\left[\frac{1}{\mu_0^{\Phi}}\right]-\frac{A+1}{2}\mathbb{E}\left[\frac{1}{1+A\eta\mu_0^{\Phi}(1-\epsilon)}\right]+\frac{A+1}{2}, \tag{23}$$

where the distribution of μ_0^{Φ} is given in (12).

Remark 1. *When $\epsilon=0$, (23) reduces to the network average AoI under TSA without feedback failure; when $\epsilon=1$, the result in (23) corresponds to that in a pure SA scenario. To this end, we conclude that in the presence of ACK feedback error, the network average AoI under the TSA protocol is a combination of those under TSA without ACK error and SA, whereas the effect is analytically characterized in (23).*

Remark 2. *If we consider the destination nodes are always active, using the result in [17], the ACK feedback failure probability can be calculated as follows:*

$$\begin{aligned}\epsilon&=1-2\pi\lambda_{\mathrm{d}}\\&\times\int_0^{\infty}\exp\left(-\pi\lambda_{\mathrm{d}}r^2-\tau r^{\alpha}-2\pi\lambda_{\mathrm{d}}\int_r^{\infty}\frac{\tau x}{\tau+(\frac{x}{r})^{\alpha}}\mathrm{d}x\right)r\mathrm{d}r,\end{aligned} \tag{24}$$

where τ is the decoding threshold for ACK feedback. In this case, ϵ is positively correlated with destination node density and ACK decoding threshold.

We present the convergence behavior of (23) under different ACK feedback failure probability in Fig. 4, which reveals that the network average AoI converges rapidly during the iterations process. Moreover, as the ACK feedback failure probability increases, more iterations are required for network average AoI convergence.

IV. Numerical Results

In this section, we conduct simulations to verify the theoretical derivations. Then, we use the analytical results to explore the effect of ACK feedback failure probability on the network average AoI under different network configurations. Specifically, before each simulation run, we set source nodes and destination nodes to be randomly distributed over a unit area of 100×100 square based on independent PPPs. The simulation time is set to 10^6 time slots. The AoI for each destination is recorded for each time slot, and then averaged to obtain the network average AoI performance for each simulation. This process is repeated 1000 times to compute the final performance metric. Unless otherwise specified, we use the following parameters: $\alpha=3.8$, $\theta=0$ dB, $\lambda_{\mathrm{d}}=0.001$.

Fig. 5 displays the network average AoI evaluated under simulations and analysis, where the network average AoI is

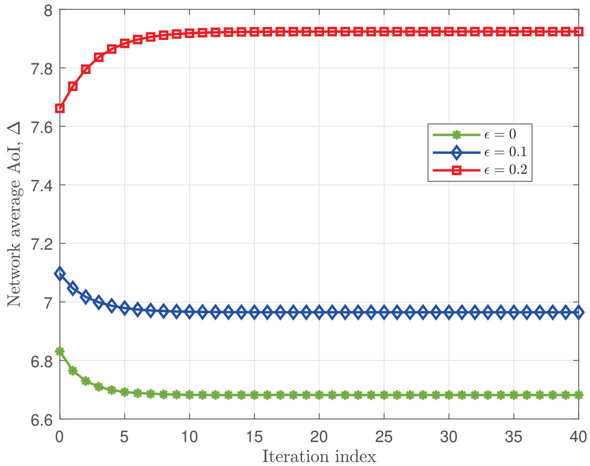

Fig. 4: Convergence behavior of network average AoI under different ACK feedback failure probability, in which we set $\eta = 0.8$, $\frac{\lambda_s}{\lambda_d} = 2$ and $A = 10$.

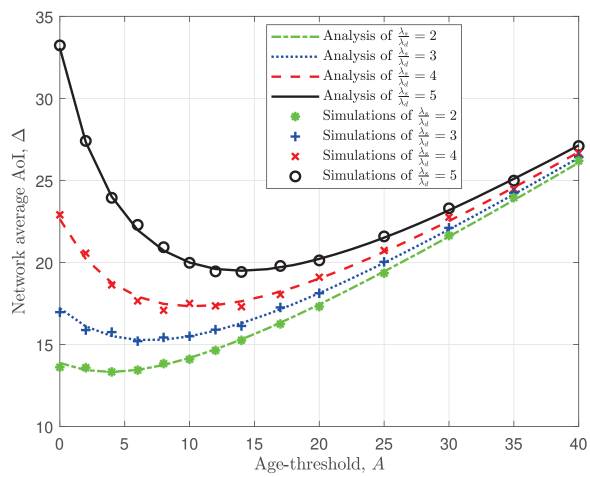

Fig. 5: Network average AoI versus age-threshold under different deployment densities ratio with imperfect ACK feedback, in which we set $\eta = 0.1$, $\epsilon = 0.2$ and $\frac{\lambda_s}{\lambda_d} \in \{2, 3, 4, 5\}$.

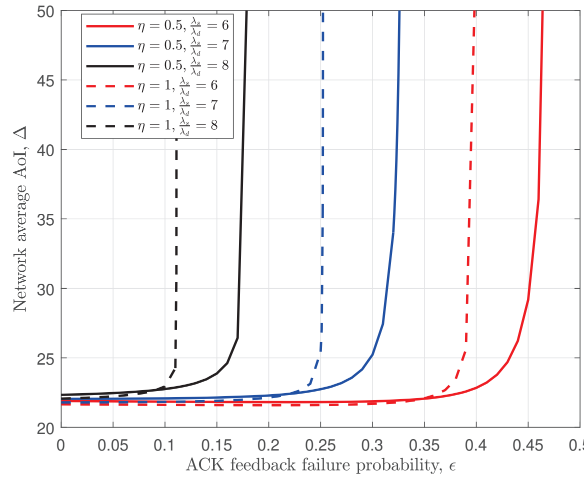

(a)

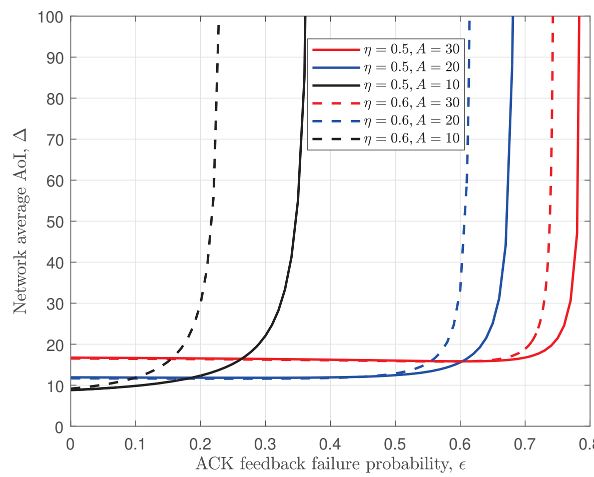

(b)

Fig. 6: Network average AoI versus ACK feedback failure probability under different deployment density ratio and age threshold: (a) $A = 40$, $\frac{\lambda_s}{\lambda_d} = \{5, 6, 7\}$, $\eta = \{0.4, 0.5\}$, (b) $\frac{\lambda_s}{\lambda_d} = 3$, $A \in \{10, 20, 30\}$, $\eta = \{0.5, 0.6\}$.

depicted as a function of age threshold under different deployment densities. From this figure, we confirm the accuracy of our derivations by observing the close match between the analysis and simulation results. We also notice that optimal age thresholds still exist that minimize the network average AoI under various deployment conditions.

Fig. 6(a) illustrates the relationship between the network average AoI and ACK feedback failure probability under different deployment densities ratios and update rates. In Fig. 6(a), we notice that when the deployment density ratio is relatively low, the interference between source nodes is weak, and the network average AoI will remain stable even the ACK feedback failure probability increases. However, when the deployment density ratio is relatively high, due to the severe interference among source nodes, its network average AoI cannot maintain stable with the increase of ACK feedback failure probability. Similar to Fig. 6(a), in Fig. 6(b), under the same deployment density ratio and age-threshold, with the increase of update rate, network average AoI under TSA with imperfect ACK feedback becomes sensitive to the ACK feedback failure probability. Considering both figures, the network average AoI becomes more sensitive to the ACK feedback failure probability when the network has higher concurrency and severe interference.

In Fig. 7, we use (23) and the exhaustive search algorithm to obtain the optimal network average AoI under different deployment densities with optimal update rate and age threshold. It is evident from this figure that when ACK feedback decoding errors occur, regardless of how the update rate and

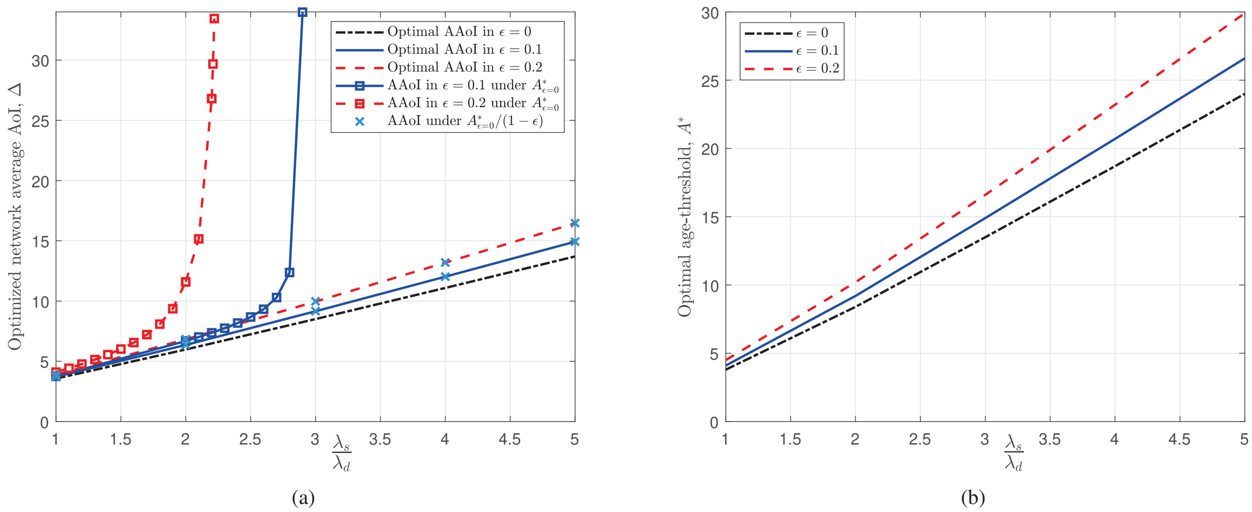

Fig. 7: Optimized network average AoI and age-threshold versus deployment density ratio under various ACK feedback failure probability: (a) optimized network average AoI, (b) optimal age-threshold.

age threshold are adjusted, the optimal network average AoI will experience a performance loss compared to the error-free case. The performance loss will become more significant when the ACK feedback failure probability, and the density of source node increase, due to the decreasing capability of TSA which relies on accurate ACK feedback in reducing interference and equalize the update interval are discount. Moreover, it also shows that the optimal age threshold to achieve the optimal network average AoI increases as the ACK feedback failure probability is exacerbated. Thus, increasing the age threshold appropriately can help reduce the performance loss caused by ACK feedback errors. However, it still remains slightly worse than in the perfect ACK feedback scenario.

V. Conclusion

In this paper, we developed an analytical framework for understanding the role of ACK feedback in TSA-like status updating protocol on the AoI performance. Our analysis revealed that when there is a positive probability of ACK feedback failure, the TSA protocol reduces to a hybrid of the TSA under perfect ACK feedback and SA protocols, leading to an increase in node concurrency and a reduced function of TSA to equalize the update intervals, resulting in a performance loss of average network AoI performance limits. While increasing the age threshold appropriately can help mitigate this performance loss, it still remains slightly worse than in the perfect ACK feedback scenario. Our analysis highlights the importance of the ACK feedback in the TSA protocol.

Appendix

A. Proof of Theorem 1

We begin by caculating the m-th moment of transmission success probability, as given in (25), where step (a) utilizes the probability generating functional (PGFL) of a PPP, while step (b) follows from the application of the binomial theorem. In step (c), we use the Beta function to simplify the integral, leading to the following expression:

$$\int_0^\infty \frac{v}{\left(1+\frac{v^\alpha}{\theta\|x_0\|^\alpha}\right)^k}\mathrm{d}v = \frac{\|x_0\|^2\theta^{\frac{2}{\alpha}}}{\alpha}B\left(\frac{2}{\alpha}, k-\frac{2}{\alpha}\right). \quad (26)$$

In step (d), we compute the expectation over the distance x_0, based on the refined distance distribution in cellular network [18]

$$f_R(r) = \frac{5}{2}\pi\lambda_\mathrm{d} r e^{-\frac{5}{4}\lambda_\mathrm{d}\pi r^2}, \quad (27)$$

and the result in step (f) is obtained through $\int_0^\infty x e^{-ax^2}dx = \frac{1}{2a}$, and further algebraic manipulations.

Finally, using the Gil-Pelaez theorem [19], we derive the cumulative distribution function (CDF) of μ_0^Φ as:

$$F(u) = \frac{1}{2} - \frac{1}{\pi}\int_0^\infty \mathrm{Im}\left\{u^{-j\omega}\mathbb{E}\left[\left(\mu_0^\Phi\right)^{j\omega}\right]\right\}\frac{\mathrm{d}\omega}{\omega}. \quad (28)$$

Then, the CDF of the transmission success probability in Theorem 1 is obtained by substituting (25) into above equation.

References

[1] N. Pappas, M. A. Abd-Elmagid, B. Zhou, W. Saad, and H. S. Dhillon, *Age of Information: Foundations and Applications*. Cambridge University Press, 2022.

[2] Y. Sun, I. Kadota, R. Talak, and E. Modiano, *Age of information: A new metric for information freshness*. Springer Nature, 2022.

[3] S. Kaul, R. Yates, and M. Gruteser, "Real-time status: How often should one update?," in *Proc. IEEE INFOCOM, Orlando, FL, USA*, pp. 2731–2735, Mar. 2012.

[4] X. Sun, F. Zhao, H. H. Yang, W. Zhan, X. Wang, and T. Q. S. Quek, "Optimizing age of information in Random-Access Poisson Networks," *IEEE Internet Things J.*, vol. 9, no. 9, pp. 6816–6829, Sep. 2022.

[5] R. D. Yates and S. K. Kaul, "Status updates over unreliable multiaccess channels," in *Proc. IEEE Int. Symp. Inf. Theory (ISIT), Aachen, Germany*, pp. 331–335, Jun. 2017.

$$
\begin{aligned}
\mathbb{E}\left[\left(\mu_0^{\Phi}\right)^m\right] &= \mathbb{E}\left[\prod_{i\neq 0}\left(1-\frac{\frac{\eta}{1+A\eta\mu_0^{\Phi}(1-\epsilon)}}{1+\frac{\|x_i\|^\alpha}{\theta\|x_0\|^\alpha}}\right)^m\right] \\
&\overset{(a)}{=} \mathbb{E}\left[\exp\left(-\lambda_{\mathrm{s}}\int_{x\in\mathbb{R}^2}\left(1-\mathbb{E}\left[\left(1-\frac{\frac{\eta}{1+A\eta\mu_0^{\Phi}(1-\epsilon)}}{1+\frac{\|x\|^\alpha}{\theta\|x_0\|^\alpha}}\right)^m\right]\right)\mathrm{d}x\right)\right] \\
&\overset{(b)}{=} \mathbb{E}\left[\exp\left(-2\pi\lambda_{\mathrm{s}}\int_0^\infty\sum_{k=1}^m\binom{m}{k}\frac{(-1)^{k+1}\mathbb{E}\left[\left(\frac{\eta}{1+A\eta\mu_0^{\Phi}(1-\epsilon)}\right)^k\right]}{\left(1+\frac{v^\alpha}{\theta\|x_0\|^\alpha}\right)^k}v\mathrm{d}v\right)\right] \\
&\overset{(c)}{=} \mathbb{E}\left[\exp\left(-\frac{2\pi\lambda_{\mathrm{s}}\|x_0\|^2\theta^{\frac{2}{\alpha}}}{\alpha}\sum_{k=1}^m\binom{m}{k}(-1)^{k+1}\mathbb{E}\left[\left(\frac{\eta}{1+A\eta\mu_0^{\Phi}(1-\epsilon)}\right)^k\right]B\left(\frac{2}{\alpha},k-\frac{2}{\alpha}\right)\right)\right]. \\
&\overset{(d)}{=} \int_0^\infty\exp\left(-\frac{2\pi\lambda_{\mathrm{s}}r^2\theta^{\frac{2}{\alpha}}}{\alpha}\sum_{k=1}^m\binom{m}{k}(-1)^{k+1}\mathbb{E}\left[\left(\frac{\eta}{1+A\eta\mu_0^{\Phi}(1-\epsilon)}\right)^k\right]B\left(\frac{2}{\alpha},k-\frac{2}{\alpha}\right)\right)\cdot\frac{5}{2}\pi\lambda_{\mathrm{d}}re^{-\frac{5}{4}\lambda_{\mathrm{d}}\pi r^2}\,\mathrm{d}r \\
&\overset{(f)}{=} \frac{1}{1+\frac{\frac{8}{5}\lambda_{\mathrm{s}}\theta^{\frac{2}{\alpha}}}{\lambda_{\mathrm{d}}\alpha}\sum_{k=1}^m\binom{m}{k}(-1)^{k+1}\mathbb{E}\left[\left(\frac{\eta}{1+A\eta\mu_0^{\Phi}(1-\epsilon)}\right)^k\right]B\left(\frac{2}{\alpha},k-\frac{2}{\alpha}\right)}. \qquad (25)
\end{aligned}
$$

[6] H. H. Yang, A. Arafa, T. Q. S. Quek, and H. V. Poor, “Optimizing Information Freshness in Wireless Networks: A Stochastic Geometry Approach,” *IEEE Trans. Mobile Comput.*, vol. 20, no. 6, pp. 2269–2280, Jun. 2021.

[7] H. H. Yang, C. Xu, X. Wang, D. Feng, and T. Q. S. Quek, “Understanding Age of Information in Large-Scale Wireless Networks,” *IEEE Trans. Wireless Commun.*, vol. 20, no. 5, pp. 3196–3210, May 2021.

[8] H. H. Yang, M. Song, C. Xu, X. Wang, and T. Q. S. Quek, “Locally Adaptive Status Updating for Optimizing Age of Information in Poisson Networks,” *IEEE Trans. Mobile Comput.*, vol. 22, no. 12, pp. 7343–7354, Dec. 2023.

[9] Z. Yue, H. H. Yang, M. Zhang, and N. Pappas, “Age of Information Under Frame Slotted ALOHA-Based Status Updating Protocol,” *IEEE J. Sel. Areas Commun.*, vol. 41, no. 7, pp. 2071–2089, May 2023.

[10] Y. Sun, E. Uysal-Biyikoglu, R. D. Yates, C. E. Koksal, and N. B. Shroff, “Update or wait: How to keep your data fresh,” *IEEE Trans. Inf. Theory*, vol. 63, no. 11, pp. 7492–7508, Nov. 2017.

[11] H. Chen, Y. Gu, and S.-C. Liew, “Age-of-Information Dependent Random Access for Massive IoT Networks,” in *Proc. IEEE INFOCOM Workshops, Toronto, Canada*, pp. 930–935, Jul. 2020.

[12] X. Chen, K. Gatsis, H. Hassani, and S. S. Bidokhti, “Age of Information in Random Access Channels,” *IEEE Trans. Inf. Theory*, vol. 68, no. 10, pp. 6548–6568, Jun. 2022.

[13] M. Ahmetoglu, O. T. Yavascan, and E. Uysal, “MiSTA: An Age-Optimized Slotted ALOHA Protocol,” *IEEE Internet of Things J.*, vol. 9, no. 17, pp. 15484–15496, May 2022.

[14] M. Moradian, A. Dadlani, A. Khonsari, and H. Tabassum, “Age-Aware Dynamic Frame Slotted ALOHA for Machine-Type Communications,” *IEEE Trans. Commun.*, vol. 72, no. 5, pp. 2639–2654, May 2024.

[15] H. H. Yang, N. Pappas, T. Q. S. Quek, and M. Haenggi, “Analysis of the Age of Information in Age-Threshold Slotted ALOHA,” in *Int. Symposium Modeling and Optimization in Mobile, Ad Hoc, and Wireless Networks (WiOpt), Singapore*, pp. 366–373, Aug. 2023.

[16] F. Zhao, N. Pappas, C. Ma, X. Sun, T. Q. S. Quek, and H. H. Yang, “Age-Threshold Slotted ALOHA for Optimizing Information Freshness in Mobile Networks,” *to appear in IEEE Trans. Wireless Commun.*

[17] J. G. Andrews, A. K. Gupta, and H. S. Dhillon, “A Primer on Cellular Network Analysis Using Stochastic Geometry,” *ArXiv*, vol. abs/1604.03183, 2016.

[18] Y. Wang, M. Haenggi, and Z. Tan, “The Meta Distribution of the SIR for Cellular Networks With Power Control,” *IEEE Trans. on Commun.*, vol. 66, no. 4, pp. 1745–1757, Apr. 2018.

[19] J. GIL-PELAEZ, “Note on the inversion theorem,” *Biometrika*, vol. 38, pp. 481–482, Dec. 1951.